An Attractive "Cis-Effect" of Hydride on Neighbor Ligands: Experimental and Theoretical Studies on the Structure and Intramolecular Rearrangements of $Fe(H)_2(\eta^2\text{-}H_2)(PEtPh_2)_3$

Lori S. Van Der Sluys,[†] Juergen Eckert,[‡] Odile Eisenstein,*[,§] John H. Hall,[‡] John C. Huffman,[†] Sarah A. Jackson,[§] Thomas F. Koetzle,[⊥] Gregory J. Kubas,[‡] Phillip J. Vergamini,[‡] and Kenneth G. Caulton*[,†]

Contribution from the Department of Chemistry, Indiana University, Bloomington, Indiana 47405, Los Alamos National Laboratory, Los Alamos, New Mexico 87545, Brookhaven National Laboratory, Upton, New York 11973, and Laboratoire de Chimie Théorique, Bâtiment 490, Centre de Paris-Sud 91405, Orsay, France. *Received October 16, 1989*

Abstract: The compound of formula $FeH_4(PEtPh_2)_3$ has been established by neutron diffraction to possess the structure and linkage *cis,mer*-$Fe(H)_2(H_2)(PEtPh_2)_3$, and thus be generally similar in structure to *cis,mer*-$Fe(H)_2(N_2)(PEtPh_2)_3$, whose structure has been determined by X-ray diffraction. The Fe–hydride distances in $Fe(H)_2(H_2)(PEtPh_2)_3$ are 1.538 (7) Å (trans to H_2) and 1.514 (6) Å (trans to $PEtPh_2$), and the Fe–H (of H_2) distances are 1.607 (8) and 1.576 (9) Å. The H–H distance in coordinated dihydrogen is 0.821 (10) Å, but the H–H bond adopts an orientation unique among structurally characterized octahedral H_2 complexes: staggered with respect to the cis Fe–P and Fe–H axes. Vibrational frequencies of the $Fe(H)_2(H_2)$ substructure have been measured by *difference* inelastic neutron scattering spectroscopy. Neutron scattering also reveals the low-frequency rotational tunneling splitting, allowing estimation of the height of the torsional barrier for coordinated H_2 rotating about its midpoint (~1 kcal/mol). Molecular mechanics calculations predict a ground-state structure where the H–H bond eclipses the P–Fe–P direction. Extended Hückel calculations with conventional hydrogen parameters predict a structure where the H–H bond eclipses the P–Fe–P vector. However, if the hydridic character of the hydride center is considered in the calculations, the experimental conformation is found to be the most stable one. The extended Hückel results are analyzed to reveal the importance of a stabilizing overlap between the filled Fe–H σ orbital and the empty $\sigma^*_{H\text{-}H}$. This nascent H/H_2 bond formation is proposed to facilitate the hydride/H_2 fluxionality of $Fe(H)_2(H_2)(PEtPh_2)_3$, in part by avoiding an intermediate with four independent hydride ligands. Crystal data for $Fe(H)_2(H_2)(PEtPh_2)_3$ (27 K): a = 21.527 (5) Å, b = 11.753 (5) Å, c = 31.034 (7) Å, β = 112.09 (1)°, and Z = 8 in space group $C2/c$. Crystal data for $Fe(H)_2(N_2)(PEtPh_2)_3$ (118 K): a = 18.355 (7) Å, b = 12.227 (3) Å, c = 19.273 (8) Å, β = 118.48 (1)°, and Z = 4 in space group $P2_1/n$.

The field of transition-metal polyhydride chemistry, MH_aL_b ($a \geq 3$), has taken on additional complexity with the discovery and the evident generality that two hydride ligands can be in thermal equilibrium with, or can find greater stability as, an intact H_2 molecule coordinated to a metal. Formally, an internal redox reaction is implicated by the $M^n(H)_2 \rightarrow M^{n-2}(H_2)$ conversion, although actual oxidation changes probably are much lower. While guiding principles are few in number,[1] H_2 complexes seem to be favored (or possible) when an octahedral d^6 metal electronic configuration is created, or when the alternative dihydride would have a "very high" metal oxidation state. Thus, one frequent source of an H_2 ligand is via the protonation of a hydride complex of a metal already in a relatively high oxidation state (eq 1–3).

$$OsH_4P_3 + H^+ \rightarrow Os(H_2)H_3P_3^+ \text{ or } Os(H_2)_2HP_3^+ \quad (1)^{2b}$$

$$IrH_3P_3 + H^+ \rightarrow Ir(H_2)(H)_2P_3^+ \quad (2)^3$$

$$IrH_5P_2 + H^+ \rightarrow Ir(H_2)_2(H)_2P_2^+ \quad (3)^4$$

The compound reported by Aresta et al.[5] to have the formula $FeH_4(PEtPh_2)_3$ is a natural extension of the series $OsH_4(PMe_2Ph)_3$.[2] $RuH_4(PPh_3)_3$.[6] While a neutron diffraction structure determination of the solid osmium compound has revealed it to be an authentic tetrahydride, such a structure would leave the iron analogue in an unusually high oxidation state for a 3d metal (and in the presence of "reducing" H^- ligands!). Aresta et al. noted one anomalous infrared absorption in $FeH_4(PEtPh_2)_3$ (2380 cm^{-1}). This band has been reassigned by Crabtree and Hamilton[7] as ν(H–H) of an intact dihydrogen ligand in a report that proposed an $Fe(H)_2(H_2)(PEtPh_2)_3$ structure based upon a short T_1 relaxation time (24 ms at 250 K and 250 MHz) for (all) the FeH_4 ligands. Since this molecule is fluxional (one ^1H NMR signal is observed for all four metal-bound hydrogens at low temperature), no unambiguous determination of the detailed stereochemistry and H–H bonding is yet available. We report here the results of our studies on both $FeH_4(PEtPh_2)_3$ and $Fe(H)_2(N_2)(PEtPh_2)_3$, including a neutron diffraction structure determination of the former.

Experimental Section

General. All manipulations were carried out under a pre-purified atmosphere of the indicated gas with standard Schlenk, drybox, and glovebag techniques. Solvents were dried and deoxygenated with use of conventional procedures. Anhydrous $FeCl_2$, $PEtPh_2$, and $NaBH_4$ were obtained commercially, used without further purification, and kept under Ar or N_2. ^1H NMR spectra were recorded on a Nicolet NT-360 spectrometer and referenced to Me_4Si. ^{31}P NMR spectra were recorded on a Varian XL-100 spectrometer and referenced externally to 85% H_3PO_4. IR spectra were recorded on a Perkin-Elmer 283 spectrophotometer and referenced to polystyrene at 1601 cm^{-1}.

Synthesis. $Fe(H)_2(H_2)(PEtPh_2)_3$. The complex was made by a modification of the method of Aresta et al.[5] All solvents must be saturated with H_2 prior to use, and *all* manipulations were carried out under H_2. Use of Ar results in lower yields and impure product. N_2 gas reacts irreversibly to give $Fe(H)_2(N_2)(PEtPh_2)_3$.[8,9]

$FeCl_2$ (0.82 g, 6.5 mmol) was partially dissolved in 40 mL of H_2-saturated EtOH in a 250-mL flask, and $PEtPh_2$ (3.3 g, 2.6 mL, 15 mmol)

[†] Indiana University.
[‡] Los Alamos National Laboratory.
[§] Centre de Paris-Sud 91405.
[⊥] Brookhaven National Laboratory.

(1) (a) Jean, Y.; Eisenstein, O.; Volatron, F.; Maouche, B.; Sefta, F. *J. Am. Chem. Soc.* **1986**, *108*, 6587. (b) Hay, P. J. *J. Am. Chem. Soc.* **1987**, *109*, 705. (c) For a review article, see: Kubas, G. J. *J. Acc. Chem. Res.* **1988**, *21*, 120. Crabtree, R. H. *Adv. Organomet.* **1988**, *28*, 299.
(2) (a) Hart, D. W.; Bau, R.; Koetzle, T. F. *J. Am. Chem. Soc.* **1977**, *99*, 7557. (b) Johnson, T. J.; Huffman, J. C.; Caulton, K. G.; Jackson, S. A.; Eisenstein, O. *Organometallics* **1989**, *8*, 2073.
(3) Lundquist, E. G.; Huffman, J. C.; Folting, K.; Caulton, K. G. *Angew. Chem., Int. Ed. Engl.* **1988**, *27*, 1165.
(4) Crabtree, R. H.; Lavin, M. *J. Chem. Soc., Chem. Commun.* **1985**, 1661.
(5) Aresta, M.; Giannoccaro, P.; Rossi, M.; Sacco, A. *Inorg. Chim. Acta* **1971**, *5*, 115.
(6) Linn, D. E.; Halpern, J. *J. Am. Chem. Soc.* **1987**, *109*, 2974.
(7) Crabtree, R. H.; Hamilton, D. G. *J. Am. Chem. Soc.* **1986**, *108*, 3124.
(8) Sacco, A.; Aresta, M. *J. Chem. Soc., Chem. Commun.* **1968**, 1223.
(9) Aresta, M.; Giannoccaro, P.; Rossi, M.; Sacco, A. *Inorg. Chim. Acta* **1971**, *5*, 203.

0002-7863/90/1512-4831$02.50/0

Table I. Crystallographic Data for $Fe(H)_2N_2(PEtPh_2)_3$

chemical formula	$C_{42}H_{47}P_3N_2Fe$	space group	$P2_1/n$
a, Å	18.355 (7)	T, °C	−155
b, Å	12.227 (3)	λ, Å	0.71069
c, Å	19.273 (8)	ρ_{calcd}, g cm^{-3}	1.273
β, deg	118.48 (1)	μ(Mo Kα), cm^{-1}	5.5
V, Å^3	3802.04	R	0.0495
Z	4	R_w	0.0475
formula wt	728.6		

was added by syringe. A white precipitate formed, and the slurry was cooled to 0 °C in an ice bath.[10] $NaBH_4$ (0.80 g, 21 mmol) was slowly added to the slurry over 30 min, during which time H_2 gas evolution was accompanied by a color change to brown and then red-orange. The ice bath was then removed, and H_2 was bubbled through the solution for the remainder of the reaction period. After ca. 2 h a thick bright-yellow precipitate had formed: after 5 h cessation of gas evolution indicated completion of the reaction. The solid yellow product was collected on a coarse fruit, washed with 7 × 5 mL of EtOH, and extracted from a dark, insoluble solid with a minimum amount of toluene (~3 mL). EtOH (double the volume of toluene employed, or ~6 mL) was layered on top of the toluene solution, and the flask was placed in the freezer at −20 °C. Large clusters of yellow plates began to form after a few days. These were isolated by removal of the mother liquor with a cannula and drying in a stream of H_2. Often an amorphous, insoluble brown powder formed along with the crystals; this powder resulted in broadened NMR spectra. It was easily removed by dissolution of the crystals in toluene and filtration or quick washing with cold EtOH.

^{1}H NMR (25 °C, C_6D_6): δ −11.7 (q, J_{HP} = 26.9 Hz, FeH), 0.95 (m, CH_2CH_3), 1.89 (m, CH_2CH_3), 7.00 (m, m- and p-phenyl), 7.52 (m, o-phenyl). Hydride-coupled ^{31}P NMR (25 °C, C_6D_6): δ 73.92 (quint, J_{PH} = 20.6 Hz). IR (25 °C, Fluorolube, cm^{-1}): ν(FeH_2) = 2380 (m), ν(FeH) = 1930 (m), 1865 (m).

$Fe(H)_2(N_2)(PEtPh_2)_3$. (A) A solution of $FeH_4(PEtPh_2)_3$ (benzene-d_6, 25 °C, ca. 30 mg per 2 mL) was placed (without stirring) under 1 atm of N_2 overnight, resulting in a yellow-brown suspension containing $FeH_2N_2(PEtPh_2)_3$ as well as other unidentified impurities.[11] The product was characterized by its ^{31}P{^{1}H} NMR[12] and IR spectra[8,9] and by the presence of two new hydride multiplets in the ^{1}H NMR; the broad AB_2XY pattern is contrary to the hydride pattern reported by Aresta and is similar to that of $(H)_2Ru(N_2)(PPh_3)_3$.[13] Due to the instability of $Fe(H)_2(N_2)(PEtPh_2)_3$, the alkyl region of the ^{1}H NMR spectrum consistently contained resonances of unidentified impurities, along with those resonances of the nitrogen complex.

(B) Exposure of 30 mg of $FeH_4(PEtPh_2)_3$ (benzene-d_6, 25 °C) under H_2 to 10 μL of air overnight resulted in a 1:1 mixture of the reagent and the dinitrogen complex (as shown by ^{1}H NMR), along with an unidentified insoluble brown powder. Exposure of $FeH_4(PEtPh_2)_3$ to 1 atm of air resulted in complete decomposition to intractable products.

^{1}H NMR (25 °C, C_6D_6): δ −11.2 (m, FeH), −16.2 (m, FeH), 0.67 (br), 1.06 (br), 1.80 (br), 2.19 (br), 2.37 (br), 7.10 (br), 7.50 (br), 7.66 (br). ^{31}P {^{1}H} NMR (25 °C, C_6D_6): δ 69.4 (d, 2 P, J_{PP} = 15 Hz), 61.8 (t, 1 P). IR (25 °C, Fluorolube, cm^{-1}): ν(NN) = 2043 (vs), ν(FeH) = 1950 (m), 1850 (m).

X-ray Structure Determination of $Fe(H_2)(N_2)(PEtPh_2)_3$. An orange needle was selected, cleaved, and transferred to a goniostat with use of standard inert atmosphere (N_2) handling techniques and cooled to −155 °C for characterization and data collection. A systematic search of a limited hemisphere of reciprocal space located a set of diffraction maxima with monoclinic symmetry and systematic absences corresponding to the unique space group $P2_1/n$. Subsequent solution and refinement of the structure confirmed this centrosymmetric choice. Data were collected in the usual manner[14] with use of a continuous θ–2θ scan ($6° \le 2\theta \le 45°$) with fixed backgrounds. Parameters of the unit cell and data collection appear in Table I. Data were reduced to a unique set of intensities and associated esd's in the usual manner. The structure was solved by a combination of direct methods (MULTAN78) and Fourier techniques. The positions of all hydrogen atoms were clearly visible in a difference Fourier phased on the non-hydrogen atoms, and the coordinates and isotropic thermal parameters for hydrogens were varied in the final cycles of refinement. A final difference Fourier was essentially featureless, with the largest peak being 0.53 e/Å^3. Since the crystal was small (0.24 × 0.24 × 0.32 mm) and nearly spherical in shape, no absorption correction was deemed necessary.

The results of the structure determination are shown in Table II and Figure 1.

X-ray Diffraction Structure of $FeH_4(PEtPh_2)_3$. A single-crystal X-ray diffraction structure determination of $FeH_4(PEtPh_2)_3$ was carried out at −155 °C. With use of 4752 reflections ($6° \le 2\theta \le 50°$) whose F exceeded $3\sigma(F)$, the structure model refined to $R(F)$ = 0.0576 and $R_w(F)$

Table II. Selected Bond Distances (Å) and Angles (deg) for Two Fe(II) Hydrides

	$Fe(H)_2(H_2)(PEtPh_2)_3$	$Fe(H)_2(N_2)(PEtPh_2)_3$
Fe–P1	2.206 (4)	2.207 (1)
Fe–P2	2.174 (4)	2.213 (2)
Fe–P3	2.162 (5)	2.176 (1)
Fe–H1	1.607 (8)	
Fe–H2	1.576 (9)	
Fe–H3	1.514 (6)	1.42 (4)
Fe–H4	1.538 (7)	1.43 (4)
H1–H2	0.821 (10)	
Fe–N47		1.786 (7)
N47–N48		1.136 (7)
P1–Fe–P2	97.6 (2)	105.9 (1)
P1–Fe–P3	105.3 (2)	104.7 (1)
P1–Fe–N47		97.2 (2)
P2–Fe–P3	149.8 (2)	148.9 (1)
P2–Fe–N47		89.0 (2)
P3–Fe–N47		93.3 (2)
Fe–N47–N48		179.3 (5)
P1–Fe–H3	177.7 (3)	157.7 (16)
P1–Fe–H4	93.9 (3)	78.8 (17)
P2–Fe–H3	83.6 (3)	74.0 (17)
P2–Fe–H4	79.4 (3)	92.6 (16)
P3–Fe–H3	74.2 (3)	75.5 (17)
P3–Fe–H4	79.7 (3)	87.3 (16)
N47–Fe–H3		105.1 (16)
N47–Fe–H4		176.0 (17)
H3–Fe–H4	88.2 (3)	78.9 (22)
P1–Fe–H1	82.4 (3)	
P1–Fe–H2	104.0 (4)	
P2–Fe–H1	111.6 (4)	
P2–Fe–H2	88.2 (4)	
P3–Fe–H1	91.0 (4)	
P3–Fe–H2	104.6 (5)	
H1–Fe–H2	29.9 (4)	
H1–Fe–H3	95.4 (4)	
H1–Fe–H4	168.8 (5)	
H2–Fe–H3	74.1 (5)	
H2–Fe–H4	159.5 (5)	

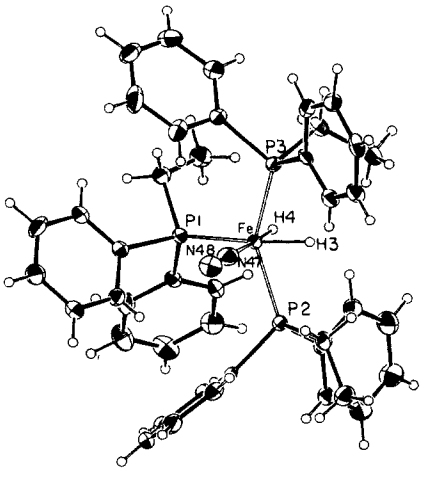

Figure 1. ORTEP drawing of $Fe(H)_2N_2(PEtPh_2)_3$ oriented as in Figure 2, to show mutual similarities and differences. Selected atom labeling is shown.

(10) Omission of the ice bath caused the $NaBH_4$ to react too rapidly with the $FeCl_2$; no recrystallized product was obtained from the resultant green-brown solution.

(11) Stirring of the reaction mixture resulted in decomposition of both the starting material and product, as evidenced by very broad resonances in the NMR spectra.

(12) Hydride and Ligand-Substitution Organometallic Chemistry of Zirconium and Iron. Wells, N. J. Ph.D. Thesis, Indiana University, 1983.

(13) Knoth, W. H. *J. Am. Chem. Soc.* **1972**, *94*, 104.

(14) Huffman, J. C.; Lewis, L. N.; Caulton, K. G. *Inorg. Chem.* **1980**, *19*, 2755.

Table III. Crystal Data and Experimental Details for $Fe(H)_2(H_2)(PEtPh_2)_3$ (Neutron Diffraction Study)

a, Å	21.527 (5)
b, Å	11.753 (5)
c, Å	31.034 (7)
β, deg	112.09 (1)
V, Å^3	7275 (4)
monoclinic, space group	*C*2/*c*
Z	8
T, K	27.0 (0.5)
hkl limits of measd reflctns	$-29 \le h \le 29$, $-16 \le k \le 3$, $0 \le l \le 42$
range of 2θ, deg	5–105
range of $\sin\theta/\lambda$, Å^{-1}	0.038–0.685
no. of measured reflctns	11976
no. of independent reflctns	9776
no. of reflctns, $I > 3\sigma(I)$	4764
$R(F)$ $[I > 3\sigma(I)]$	0.067
$R_w(F)$ $[I > 3\sigma(I)]$	0.056
$R(F^2)\{R_w(F^2)\}$ $[I > 3\sigma(I)]$	0.094 {0.096}
goodness of fit for all data	1.30

= 0.0553. After all carbon-bound hydrogens were located and refined (isotropic *B*'s), hydride hydrogens were also evident as peaks of 0.84, 0.80, and 0.76 e/Å^3. While there were only *three* such hydride hydrogens, *all* had reasonable *B* values (0.8 (8), 3.7 (12), and 2.8 (11) Å^2), Fe–H distances (1.48 (4), 1.36 (5), and 1.37 (5) Å^2), and angles corresponding to an octahedron. After including these three hydrides in the final refinement model, the largest residual in a difference map was 0.50 e/Å^3. Full details of the structure determination are available from the Indiana University Chemistry Library as Molecular Structure Center report No. 86008. Since the finding of only three hydride atoms was in conflict with all of our spectroscopic data taken both before and after X-ray data collection on crystals from the batch employed, we abandoned the X-ray approach to determining the character of the metal-bound hydrogen and employed neutron diffraction instead.

Neutron Diffraction Structure of $FeH_4(PEtPh_2)_3$. Large yellow plates were isolated as in the procedure described above and dried in a stream of H_2. These appeared to turn opaque and orange when dry and were stored under 1 atm of H_2.

A dark-yellow plate-like single crystal of the title compound, of overall dimensions 0.75 × 2.0 × 2.8 mm along *a**, *b**, and *c**, respectively, was mounted (halocarbon grease[15]) on an Al pin aligned approximately along [1$\bar{1}$2] and sealed in an Al container under H_2. Neutron diffraction data were measured on a four-circle diffractometer at the Brookhaven High Flux Beam Reactor, with the sample maintained at $T = 27 \pm 0.5$ K (to avoid condensation of H_2) in a closed-cycle helium refrigerator[16] and with a neutron wavelength (Ge (220) monochromator) of 1.158 82 (7) Å.[17] Unit-cell parameters, determined from mean $\sin^2\theta$ values of 16 Friedel pairs with $55° \le 2\theta \le 68°$, are given together with experimental details in Table III. Intensities of Bragg reflections were measured[18] by means of $\theta/2\theta$ step scans, with 60–90 steps per scan and counts accumulated for ca. 2 s per step, the exact counting time being determined by monitoring the incident beam intensity. The 2θ scan range was 3.0° for $5° \le 2\theta \le 60°$ and 1.2 (1.00 + 2.58 tan θ)° for $60° < 2\theta \le 105°$. Intensities of three reflections were monitored every 200 reflections during data collection to check experimental stability; analysis[19] of these monitor intensities indicated <0.6% variation in effective scale factor over the entire duration of the measurements. Integrated intensities were calculated assuming 10% of the scans at either extremity represent background; Lorentz and absorption corrections (by numerical integration[20] over a Gaussian grid of 6 × 16 × 16 points, $\mu = 0.2385$ mm^{-1}, crystal approximated by 8 boundary planes belonging to {100}, {010}, {001}, and {012}, calculated crystal volume 4.0 mm^3, minimum and maximum transmission 0.59 and 0.82, respectively) were applied. Altogether 11 976 measured intensities were reduced to 9776 independent values of F_o^2, after rejection of space group absences and averaging over the 2/*m* Laue symmetry: $R_{int} = 0.052$ for $5° \le 2\theta \le 60°$ and $R_{int} = 0.022$ for $60° < 2\theta \le 105°$. Data reduction was carried out on a micro-VAX II computer with the Uppsala package of crystallographic programs.[21] The refinement was begun with the X-ray positional parameters for the non-hydrogen atoms. All hydrogens were located in subsequent difference maps. Results of the structure determination are shown in Figure 2 and Tables II and III.

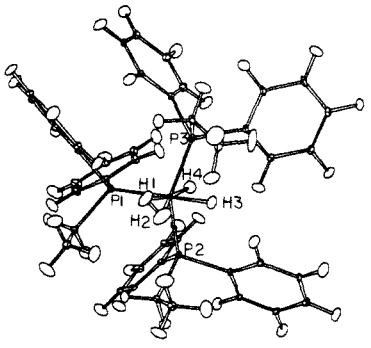

Figure 2. ORTEP drawing of $Fe(H)_2(H_2)(PEtPh_2)_3$ as determined by neutron diffraction, showing selective atom labeling.

Neutron Scattering Spectroscopy. The inelastic neutron scattering (INS) vibrational data were taken on the Filter difference spectrometer (FDS) at the Los Alamos Neutron Scattering Center[22] with use of two samples, one of which had the dihydrogen and hydride ligands deuterated. The INS spectrum of the latter was then subtracted from that of the isotopically normal sample, a procedure[23] that leaves essentially only those vibrational modes involving the dihydrogen and hydride ligands. The reason for this is that the neutron scattering cross-section for D is more than one order of magnitude less than that of H. Vibrational modes involving mainly the deuteride or D_2 ligands therefore cannot be "seen" in the presence of many more modes that include hydrogen motion, i.e., those of the phosphine ligands. The deuterated sample thus simply serves as a "blank" for subtracting out the phosphine ligand modes.

The low-frequency rotational tunneling spectra were obtained on the cold-neutron time-of-flight spectrometers IN5 and IN6 at the high flux reactor of the Institut Laue-Langevin (Grenoble, France). No "blank" sample was necessary in this case, since the other ligands would not be expected to have observable excitations in the frequency range of interest ($\le$10 cm^{-1}) of this experiment.

Molecular Mechanics Calculations. Molecular mechanics calculations were carried out with Chem-X software.[24] Atomic coordinates for $Fe(H)_2(\eta^2\text{-}H_2)(PPh_2Et)_3$ were taken from the neutron structure. After conversion to an orthonormal system, the iron atom was set at the origin. The molecule was then rotated so that the midpoint of the H_2 ligand lay along the *z* axis. The MM2 energy[25] was calculated with all bond lengths, bond angles, and torsion angles held constant ("frozen" in the ground-state values) and all atomic charges set to zero, leaving only the possibility of changing the Lennard-Jones nonbonding potentials. This calculation was repeated for 36 5° clockwise rotations of the dihydrogen molecule about the *z* axis. Additional rotations were obviated by symmetry considerations.

Results and Discussion

Solution Characterization. We find $FeH_4(PEtPh_2)_3$ to be very prone to decomposition in vacuum or in argon atmosphere to a dark solid that is insoluble in aromatic hydrocarbons, aliphatic hydrocarbons, and EtOH. This decomposition is retarded by saturating solvents with H_2 and working in an environment of 1 atm of H_2, and *all* operations reported here have been carried out

(15) Epoxy worked well but became brittle at low temperatures. Any glue containing solvents such as acetone decomposed the crystals.
(16) DISPLEX Model CS 202, Air Products and Chemicals, Inc.
(17) Calibrated on the basis of KBr, $a_0 = 6.6000$ Å at $T = 298$ K. Donnay, J. D. H., Ondik, H. M., Eds. *Crystal Data Determination Tables*, 3rd ed.; U.S. Department of Commerce and Joint Committee on Powder Diffraction Standards: Washington, DC, 1973; Vol. 2, p C-164.
(18) (a) Dimmler, D. G.; Greenlaw, N.; Kelley, M. A.; Potter, D. W.; Rankowitz, S.; Stubblefield, F. W. *IEEE Trans. Nucl. Sci.* **1976**, *NS-23*, 398–405. (b) McMullan, R. K.; Andrews, L. C.; Koetzle, T. F.; Thomas, R.; Williams, G. J. B. NEXDAS, Neutron and X-ray Data Acquisition System, unpublished work.
(19) McCandlish, L. E.; Stout, G. H.; Andrews, L. C. *Acta Crystallogr.* **1975**, *A31*, 245.
(20) Coppens, P.; Leiserowitz, L. L.; Rabinovich, D. *Acta Crystallogr.* **1965**, *18*, 1035.
(21) Lungren, J. O. *Crystallographic* Computer Programs. Report UUIC-B13-4-05; Institute of Chemistry, University of Uppsala: Uppsala, Sweden, 1982.
(22) Taylor, A. D.; Wood, E. J.; Goldstone, J. A.; Eckert, J. *J. Nucl. Inst. Methods* **1984**, *211*, 408.
(23) Eckert, J. *Physica* **1986**, *136B*, 150.
(24) Chem-X is developed and distributed by Chemical Design Ltd., Oxford, England. It was run of an Evans and Sutherland PS340 graphics workstation with a Digital Equipment Corporation VAX 11/785 (VMS Version 4.7 operating system serving as the host processor).
(25) Burkett, U.; Allinger, N. L. *Molecular Mechanics*; ACS Monograph 177; American Chemical Society: Washington, DC, 1982.

in this manner. The infrared spectrum of a mull prepared in a special wide-mouth Schlenk flask entirely under H_2 shows a band at 2380 cm^{-1}, in agreement with the report of Aresta. Since the sample used here was completely soluble in benzene, an $NaBH_4$ impurity could not be the origin of this absorption.

The ^1H NMR spectrum of $FeH_4(PEtPh_2)_3$ in C_6D_6 at 25 °C under argon shows lines significantly broader than when recorded under H_2. Under argon, the solution color is noticeably red, in comparison to the yellow of solutions under H_2. Only under H_2 is a quartet clearly resolved for the metal-bound hydrogens. The implied equivalence of the phosphine ligands is seen directly in the single $^{31}P\{^1H\}$ NMR signal observed for the sample at 25 °C; this signal splits into a quintet when the ^{31}P NMR spectrum is recorded with selective decoupling of only those hydrogens in the range 0–10 ppm. The $^{31}P\{^1H\}$ spectrum remains a singlet at −95 °C in toluene.

Variable-temperature NMR studies (−125 °C to +25 °C, methylcyclohexane-d_{14}) under H_2 showed only broadening of the hydride resonance at −100 °C.

Although ^1H and ^2H NMR experiments were carried out under a 1:1 H_2:D_2 atmosphere (25 °C, benzene-d_6 or toluene-d_8) in an attempt to observe one-bond H–D coupling, only broadening of the hydride resonance was observed. This was presumably due to an overlap of hydride resonances of the isotopomers $FeH_xD_{(4-x)}(PEtPh_2)_3$, formed by rapid scrambling of the deuterium.

Solid-State Structure. (a) $FeH_4(PEtPh_2)_3$. The neutron diffraction study produced structural parameters for the nonhydride portion of the molecule in full accord with that of the X-ray diffraction study; the geometry of the FeP_3 substructure from the two studies agrees to within 3σ. However, only the neutron diffraction study is capable of furnishing the conclusion that the molecule is correctly described as *cis,mer*-$Fe(H)_2(\eta^2\text{-}H_2)(PEtPh_2)_3$. Henceforth, only the results of the neutron diffraction study will be cited here. The quality of the neutron diffraction data makes this the most accurate determination to date of an H_2 complex. The Fe–H distances to the hydride ligands (1.514 (6) and 1.538 (7) Å) are significantly shorter than those to the dihydrogen (1.576 (9) and 1.607 (8) Å), and the dihydrogen molecule has an H–H distance of 0.821 (10) Å, which agrees with the H–H distance found in $W(H_2)(CO)_3(P(i\text{-}Pr)_3)_2$[26] and in *trans*-$[Fe(H)(H_2)(dppe)_2]BPh_4$ (dppe = $PPh_2CH_2CH_2PPh_2$).[27] The two hydride ligands are very nearly orthogonal (the H3–Fe–H4 angle is 88.2°). The shortest H–H nonbonded contacts are H2···H3 (1.862 (13) Å) and H3···H29 (1.930 (10) Å); H29 is an *o*-phenyl hydrogen on P2. The H–H vector of the dihydrogen molecule does not eclipse any other bonds in the coordination sphere. It is, instead, staggered with respect to these. The degree of rotation can be quantified with respect to either the Fe–H3–H4 plane or the P1–H3–H4 plane. Each of these planes is nearly identical, and the Fe–H1–H2 plane is rotated 43° with respect to them.

There are considerable distortions from a regular octahedron. The two cisoid P–Fe–P angles are considerably larger than 90° and are unequal (97.6 (2)° and 105.3 (2)°). Since the transoid phosphines bend toward the uncrowded $Fe(H)_2(H_2)$ portion of the coordination sphere, they subtend an angle of only 149.8 (2)°. While P2 and P3 bend identically (mean 79.5 (3)°) toward H4, P3 bends more (74.2 (3)°) toward H3 than does P2 (83.6 (3)°). The bending of P2 and P3 is *away* from the H_2 ligand. This contrasts to their bending in $Fe(H)_2(N_2)(PEtPh_2)_3$; see below. The Fe–P distance trans to hydride (2.206 (4) Å) is significantly longer than the mutually trans-disposed Fe–P distances (both are equivalent with an average value of 2.168 (6) Å).

(b) $Fe(H)_2(N_2)(PEtPh_2)_3$. The molecule exists in the cis,mer-isomeric form of an octahedron and is generally similar to (but not isomorphous with) $Fe(H)_2(H_2)(PEtPh_2)_3$. This study represents the first structure determination of a pair of compounds differing only in a replacement of N_2 by dihydrogen. The Fe–P1 distance (trans to hydride) is identical (2.207 (1) Å) with that in $Fe(H)_2(H_2)(PEtPh_2)_3$, while those cis to this phosphorus are curiously inequivalent (2.213 (2) and 2.176 (1) Å) from one another. The transoid P2–Fe–P3 angle (148.9 (1)°) is nearly identical with that of 149.8 (2)° in $Fe(H)_2(H_2)(PEtPh_2)_3$. The Fe–H distances are within 3σ of the corresponding values in $Fe(H)_2(H_2)(PEtPh_2)_3$, but they show the anticipated systematic shortening of X-ray values for a light atom bonded to a metal. A major difference is the angular distortion of P2 and P3 in the two compounds. In $Fe(H)_2(N_2)(PEtPh_2)_3$, iron and the three phosphorus nuclei are essentially coplanar (sum of P–Fe–P angles = 359.4°). In $Fe(H)_2(H_2)(PEtPh_2)_3$, these angles sum to 352.8°, due to a bending of P2 and P3 away from the H_2 ligand.

Inelastic Neutron Scattering Studies on $Fe(H)_2(H_2)(PEtPh_2)_3$. Introduction. In order to learn more about the rotational and vibrational dynamics of the dihydrogen–metal fragment we have carried out inelastic neutron scattering (INS) experiments on the title compound in the solid state at low temperature. This technique is highly sensitive to hydrogen motions because of the very large nuclear scattering cross-section for neutrons by protons as well as the characteristically large amplitude of hydrogen motions. For rotational transitions it is also important to note that since the neutron has a nuclear spin of $^1/_2$, it can cause spin flip transitions in the scatterer of $\Delta I = \pm 1$, which are, of course, forbidden in optical spectroscopy. This property makes it possible to observe directly the so-called rotational tunneling transition within the librational ground state of the H_2 rotator (as well as other rotators such as CH_3). This tunnel splitting arises from the fact that for the weakly hindered rotator the wave functions for the molecule in the two potential minima 180° apart (in the present case) can overlap. Because of the Pauli exclusion principle, the ground state must split to remove this degeneracy, which corresponds to the two orientations of the H_2 molecule. This 180° rotation corresponds to an odd permutation of identical spin $^1/_2$ particles (protons) with respect to which the ground-state wave function has to be antisymmetric. At low temperatures these are constructed from linear combinations of nuclear spin and rotational wave functions. Thus a symmetric nuclear spin wave function (for which $I = 1$) combines with an antisymmetric rotational wave function (J odd) and vice versa. These are the two "kinds" of H_2 molecules referred to as *o*- and *p*-H_2, respectively. A spin-flip neutron scattering process thereby allows direct observation of the ortho–para H_2 transition. The latter has an energy of $2B$ (where B is the rotational constant of the H_2 molecule for a free hydrogen molecule with two rotational degrees of freedom). If the H_2 is constrained to rotate in a plane as is the case for our compound, this transition has an energy of B for zero barrier and becomes rapidly smaller with increasing barrier height.

Successful experiments of this type have already been performed on several molecular hydrogen complexes.[28-30] The low-lying vibrational excitations (including the H_2 torsion) of the metal–dihydrogen group have been identified by INS for two W complexes[28,29] and for *trans*-$[FeH(H_2)(dppe)_2]BF_4$.[30] In the former case the INS results completed the assignments of all six normal modes, while in the latter case they are the only vibrational data available. In addition, high-resolution neutron scattering spectrometers were utilized in these cases to measure the rotational tunnel splitting of the librational ground state. This information was used along with the transitions to the first excited librational state (i.e., the torsion) to derive values for the barrier height hindering the dihydrogen rotations. Thus, for example, for the $(\eta^2\text{-}H_2)$ in $W(CO)_3(H_2)(PCy_3)_2$ the barrier was found to be 2.2 kcal/mol by an analysis of the INS data in terms of a simple double-minimum potential with one angular degree of freedom.[31]

(26) Kubas, G. J.; Ryan, R. R.; Swanson, B. I.; Vergamini, P. J.; Wasserman, H. *J. Am. Chem. Soc.* **1984**, *106*, 451.
(27) Ricci, J. S.; Koetzle, T. F.; Bautista, M. T.; Hofstede, T. M.; Morris, R. H.; Sawyer, J. F. *J. Am. Chem. Soc.* **1989**, *111*, 8823. Morris, R. H.; Sawyer, J. F.; Shiralian, M.; Zubkowski, J. D. *J. Am. Chem. Soc.* **1985**, *107*, 5581.
(28) Eckert, J.; Kubas, G. J.; Dianoux, A. J. *J. Chem. Phys.* **1988**, *88*, 466.
(29) Eckert, J.; Kubas, G. J.; Hay, P. J.; Hall, J. H.; Boyle, C. M. *J. Am. Chem. Soc.* In press.
(30) Eckert, J.; Blank, H.; Bautista, M. T.; Morris, R. H. *Inorg. Chem.* Submitted for publication.
(31) Pauling, L. *Phys. Rev.* **1930**, *36*, 430.

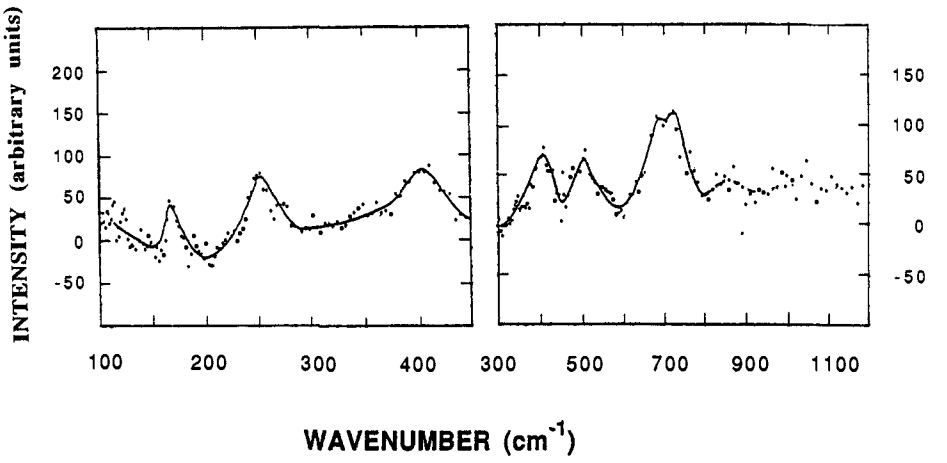

Figure 3. Difference INS vibrational spectrum of the $Fe(H_2)H_2$ fragment obtained at 15 K at the FDS at the Los Alamos Neutron Scattering Center. One peak is duplicated in both spectral regions.

Table IV. Vibrational Frequencies (cm^{-1}) with Proposed Assignments

	$FeH_2(H_2)(PPh_2Et)_3$	$Fe(CO)(NO)_2(H_2)$
$\tau(Fe(H_2))$	170, 252	
$\delta(Fe(H_2))$	405	
$\delta(Fe(H_2))$	500	
$\delta(Fe(H))$	720, 680	
$\nu_s(Fe(H_2))$	850	870
$\nu(H-H)$		2973

i.e., planar rotation of the dihydrogen ligand.

Results and Discussion

(a) Vibrational Modes. The INS vibrational spectra are shown in Figure 3 and summarized in Table IV. The relatively poor statistics of the data are the result of the subtraction procedure. Nonetheless, five features can be reasonably well identified and we attempt to assign these based primarily on comparisons with whatever other vibrational data are available. Accordingly, the two lowest frequency peaks at 170 and 252 cm^{-1} are identified as the split torsional mode, which has also been observed in the other dihydrogen complexes studied by INS. The reason for this assignment will become more apparent below. Two other deformation modes $\delta(Fe(H_2))$ remain to be assigned in the frequency range of our data, as well as the Fe–H bend for the hydride ligands and possibly $\nu_s(Fe(H_2))$. The peaks at 405 and 500 cm^{-1} are most likely the two deformation modes that occur at 460 and about 650 cm^{-1} in $W(CO)_3(H_2)(PCy_3)_2$. The doublet near 700 cm^{-1} certainly contains the Fe–H bend for the hydride, since such modes are known to fall into this range.[32] Since the Fe–H distances are different for the two chemically inequivalent hydrides (1.51 and 1.54 Å), they certainly will have slightly different values for $\delta(FeH)$, namely 680 and 720 cm^{-1} in our spectrum. This leaves $\nu_s(Fe(H_2))$ unassigned. It may well be the weak feature near 850 cm^{-1}, particularly since this mode was identified at 870 cm^{-1} in the matrix-isolated compound $Fe(CO)(NO)_2(H_2)$.[33] However, it is not obvious to what extent this compound is comparable to ours. It is, on the other hand, also possible that $\nu_s(Fe(H_2))$ is contained in the strong band at 700 cm^{-1}. This would, however, be some 250 cm^{-1} lower than in the W complex ($\nu_s(W(H_2))$ = 950 cm^{-1}), which is perhaps an unlikely large shift. Nonetheless, the vibrational data presented here for the $Fe(H_2)$ fragment suggest generally weaker metal–hydrogen interaction than in the W compound, which would imply that the H–H interaction be stronger than in the W compound ($\nu(H-H)$ = 2690 cm^{-1}). This would demand the unattractive conclusion that the broad band observed at ca. 2400 cm^{-1} in the IR for the title compound accordingly not be $\nu(H-H)$. It has been observed at 2973 cm^{-1} in $Fe(CO)(NO)_2(H_2)$, a frequency that does, of course, fall into the C–H stretching region. More extensive optical work, including the use of a fully deuterated phosphine ligand, would therefore be clearly desirable.

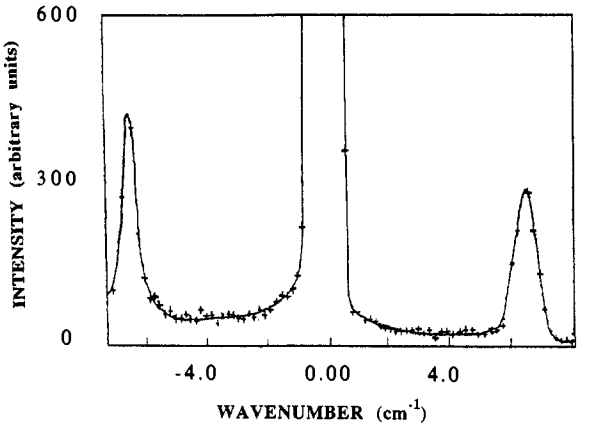

Figure 4. Rotational tunneling spectrum of the H_2 ligand in $Fe(H)_2(H_2)(PEtPh_2)_3$ obtained at 1.5 K on the INS spectrometer at the ILL.

Table V. Rotational Transitions (cm^{-1}) ($V_2 \sim 1.15$ kcal/mol)

	obsd	calcd	
		$V_2 = 7.9B$	$V_2 = 8.5B$, $V_4 = -1.7B$
"0–1"	6.4	(6.4)	(6.4)
"0–2"	170	192	184
"0–3"	252	258	238

(b) Rotational Barrier. The low-frequency rotational tunneling spectrum measured at 1.5 K on the INS spectrometer at the ILL with an incident neutron wavelength of 6 Å is shown in Figure 4. The transition is observed in both neutron energy gain and energy loss since the system will not readily relax down to the lowest level, a process that requires spin conversion for the (η^2-H_2). The value for the ground-state splitting of 6.4 cm^{-1} is the largest observed to date in molecular hydrogen complexes and implies that this system has the lowest barrier to H_2 rotation. We can derive a barrier height from this information by using only the first term of the potential for planar rotation of a dumbbell molecule:

$$V = \sum_n V_{2n}(1 - \cos(2n\Phi))/2 \qquad (4)$$

where Φ is the rotation angle about the H–Fe–(H_2) axis. Note that the Φ value where V is a minimum is not determined by this analysis. The result (Table V) is that $V_2 = 7.9B$, or 1.1 kcal/mol, if B is calculated with the H–H distance from the neutron dif-

(32) Howard, J.; Waddington, T. C. *Advances in Infrared and Raman Spectroscopy*; Clark, R. J. H., Hester, E. E., Eds.; Heyden, 1980; Vol. 7, Chapter 3.

(33) Gadd, G. E.; Upmacis, R. K.; Poliakoff, M.; Turner, J. J. *J. Am. Chem. Soc.* **1986**, *108*, 2547.

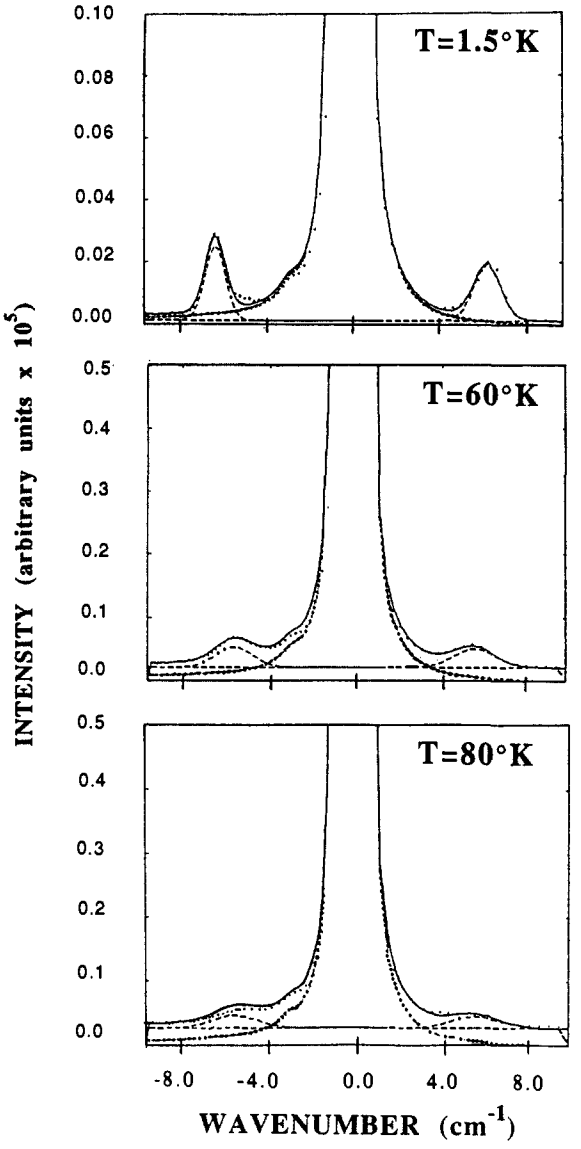

Figure 5. Temperature dependence of the rotational tunneling spectrum of the H_2 ligand in $Fe(H)_2(H_2)(PEtPh_2)_3$ obtained on the IN6 spectrometer at the ILL. The data points (small dotted line) are fitted with Lorentzians (dashed line) for the tunneling peaks and convoluted with the experimental resolution (heavy dotted line). The resulting fit is given by the solid line. The shoulder at approximately -3 cm^{-1} is an artifact of the spectrometer.

fraction experiment. With this value of V_2 one would predict the torsions to occur at 192 and 258 cm^{-1}, whereas our observations are 170 and 252 cm^{-1}. This relatively small deviation is most likely the result of the fact that the actual potential in $Fe(H)_2(H_2)(PEtPh_2)_3$ is not simply a sinusoidal function with a double-minimum. The shape of the rotational potential can be modulated by introducing more terms from eq 4. Thus, for example, a potential with $V_2 = 8.5B$ and $V_4 = -1.7B$ provides (Table V) a slightly better fit, with torsions calculated at 184 and 238 cm^{-1}. The negative V_4 term has the effect of steepening the walls while flattening the bottom of the potential well. This broadening of the energy minimum is precisely the effect deduced from Hückel calculations (see below).

The temperature dependence of the rotational tunneling peaks is shown in Figure 5. The peaks are found to broaden rapidly with temperature and shift to lower energies. The change in width and the frequency shift can be well described by Arrhenius-type relationships:[34]

$$\Gamma(T) = \Gamma_0 e^{-E(\Gamma)/kT}$$

and

$$\Delta(\hbar\omega(T)) = \hbar\omega_0 e^{-E_s/kT}$$

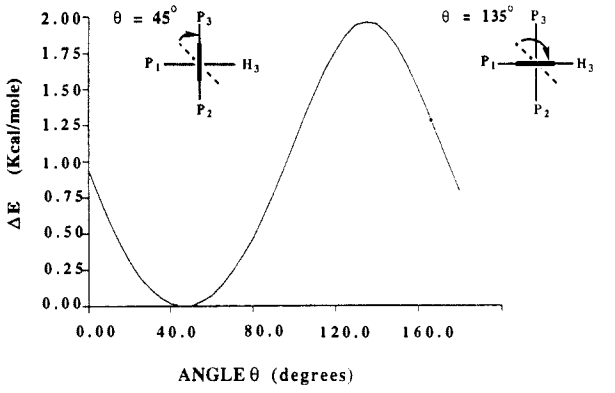

Figure 6. Molecular mechanics energy profile for rotation of the H_2 ligand (short dark line) clockwise by θ deg about the Fe–H_2 axis.

A plot of Γ and the frequency shift on a logarithmic scale vs $1/T$ shows that both are approximately described by the same activation energy, namely $E(\Gamma) \sim E_s = 80K$ (=56 cm^{-1}). This value is surprisingly low, since the theory of Hewson relates $E(\Gamma)$ to E_{01} (the transition to the first excited state), which we find at 170 cm^{-1}. A similar but not nearly as large a discrepancy was observed for the dihydrogen ligand in $W(CO)_3(H_2)(PCy_3)_2$[28] where this activation energy turned out to be approximately $^2/_3$ of the energy of the torsional mode.

The basis for the theoretical description by Hewson[34] is a perturbation treatment of a phenomenological coupling between the phonon density of states and the rotator, leading to the time-dependent correlation functions that form the neutron scattering cross-sections. The assumption for this model is that the low-frequency phonons in the solid act to distort the hindering potential of the rotator as the temperature is increased and that this results in the broadening and shift of the rotational tunneling transition peaks. The nature of this coupling between phonon modes and the rotator is not well understood, however, so that a detailed analysis for a particular system is not possible. As far as the relevance of this theory by Hewson to the dihydrogen ligands is concerned, the crucial point is likely to be that virtually all the cases of molecular rotators studied previously by neutron scattering involve INTERmolecular barriers to rotation, while in our case the barrier is entirely of INTRAmolecular origin. Thus, while it would appear reasonable that phonons (particularly low-lying optic modes) play a major role in distorting a barrier that results from interactions between molecules, this consideration would also suggest that phonons are much less important in our case, where the barrier is determined by the electronic interaction between the dihydrogen ligand and the metal and by nonbonded interactions with the other ligands on the metal. Some low-lying INTERNAL vibrational modes of the molecular hydrogen complex may well be responsible for the temperature-dependent broadening and shift of the rotational tunneling lines. A detailed understanding of this process would be extremely important for the understanding of the dynamics of the dihydrogen ligand, and in fact it may well be highly relevant to the fluxional behavior of the dihydrogen and hydride ligands at high temperatures.

Molecular Mechanics Calculation of H_2 Rotation. The molecular mechanics calculations for the $Fe(H)_2(\eta^2\text{-}H_2)(PPh_2Et)_3$ molecule show (Figure 6) a barrier of rotation due to steric effects of approximately 2 kcal/mol. Significantly, the observed crystal structure is not at a minimum steric energy in these calculations. This shows unambiguously that steric considerations alone are insufficient in this case to reproduce the experimental barrier to rotation. It was determined that the minimum steric energy configuration is alignment of the dihydrogen molecule along the P2–Fe–P3 axis (45° from the position in the crystal structure), and the maximum energy configuration corresponds to alignment of the dihydrogen molecule along the P1–Fe–H3 axis (90° from the molecular mechanics minimum). It was also found that the

(34) Hewson, A. C. *J. Phys.* **1982**, *C15*, 3855.

contributions of the hydrocarbon components of the phosphine ligands to the rotational barrier are negligible when compared to those of the hydride ligand. In fact, removing the hydrocarbon components resulted in a virtually identical plot of ΔE versus angle to that shown in Figure 6. In order to obtain information regarding the electronic component of the barrier, extended Hückel calculations were carried out.

Extended Hückel Calculations of the Rotation of H_2. In the two η^2-molecular dihydrogen complexes of d^6 ML_5 fragments structurally characterized with the accuracy of neutron diffraction,[26,27] H_2 was found to eclipse an L-M-L axis. Similar features have also been found in ethylene complexes[35] for which the bonding scheme to the metal is similar to that of molecular H_2. The title compound thus has an *unprecedented structure* in that the axis of H_2 is staggered with respect to the Fe-P and Fe-H bonds. An analysis of the bonding by theoretical means has been undertaken in order to unravel the reasons for this unique structural feature. A natural outcome of this analysis is that the factors favoring the experimental conformation give important clues to the mechanism for the compound's fluxional behavior (i.e., hydrogen/hydride site exchange).

We first discuss those factors that, in general, disfavor the staggered conformation for a regular octahedral fragment. The ideas are based on an analysis for a d^6 ML_5 olefin complex.[35a] In a complex in which the four ligands cis to the olefin are identical, the olefin π^* overlaps with either the occupied xz or yz orbitals or any linear combination of them (z along the M-olefin midpoint vector, x and y along two M-L bonds). This should lead to no rotational barrier. However, the staggered conformation is disfavored by a four-electron destabilization due to the overlap of the occupied xy with the olefin occupied π orbital as shown in **1**. The conclusion is modified when the ligands cis to the olefin are not all identical. For a d^6 complex, the olefin should eclipse preferentially the set of ligands having the inferior π accepting capability.[35b]

1

The analysis was transferred to the H_2 complex since H_2 has orbitals topologically equivalent to those of ethylene. This analysis accounts nicely for the structure of the first H_2 complex that was studied theoretically, $(CO)_3P_2W(H_2)$ (P = PH_3): H_2 eclipses the P-W-P vector despite the large steric bulk of the phosphine PCy_3. EHT[1a] and ab initio[1b] calculations confirm the preference for this conformer.

It is clear that *none of the above arguments can provide an interpretation for the unprecedented staggered structure of* $Fe(H_2)(H)_2(PEtPh_2)_3$. Some other phenomenon is at work which we shall demonstrate is directly connected with the fluxional behavior of the complex.

(a) Influence of Geometric Distortion of the Octahedral Fragment. Due to the close chemical relation between the $HFe(dppe)_2(H_2)^+$ complex, **2**, studied by Morris[27] and the present one, it is enlightening to compare both systems. We thus start with a discussion of the Morris complex, where the dihydrogen eclipses a P-Fe-P axis. Despite the fact that H_2 is now cis to four phosphines, the environment is not isotropic and H_2 eclipses a specific P-Fe-P vector. The octahedron is distorted by an unequal pinching of the two trans pairs of phosphine ligands. The smaller value P1-Fe-P3 is 166.6 (2)° (in the xz plane) while the larger one P2-Fe-P4 (in the yz plane) is 172.1 (2)° as shown schematically in **2**. According to the neutron structure, H_2 lies in the xz plane, which is the plane of the smaller P-Fe-P angle.

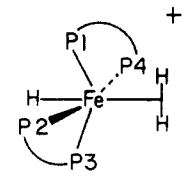

2

In order to show the importance of the structural distortion, we start by doing EHT calculations[36] on idealized octahedral (all P-Fe-P angles taken as 90°) model complex $HP_4Fe(H_2)^+$ (P = PH_3). No energy barrier was found for the rotation of H_2. In particular the staggered conformation was not found higher in energy than the eclipsed geometry. This shows that *no significant four-electron destabilization is generated in the staggered conformation.* This is a consequence of the very weak overlap between σ_{HH} and xy. The difference with the ethylene case (**1**) is simply due to the fact that π_{CC} is an orbital of greater spatial extension and directed more toward the metal xy. In other words, *no electronic factors prevent* H_2 *from adopting the staggered conformation.* However, the calculations on the model complex $HP_4Fe(H_2)^+$ (P = PH_3) using the experimental structure for $HFe(dppe)_2(H_2)^+$ show that the dihydrogen prefers to eclipse a P-Fe-P direction. The energy barrier is found to be around 2.8 kcal/mol with the preferred conformation corresponding to the neutron diffraction result. This result is due to the structural distortion away from the octahedral geometry at the metal center. The orbitals competing for σ^*_{HH} are xz and yz. As the transoid P-Fe-P angles become less than 180°, xz and yz are no longer nonbonding with respect to the phosphine lone pairs. They are destabilized in energy by mixing these lone pairs in an antibonding manner, the greater destabilization being associated with the smaller P-Fe-P angle. In addition xz and yz take on some metal p character, x and y, respectively, so that they are hybridized away from the phosphine, the greater effect again being associated with the smaller P-Fe-P angle. Therefore because of energy and overlap criteria, the orbital lying in the plane corresponding to the smaller P-Fe-P angle (xz, **3**) is the better candidate for back donation into σ^*_{HH}.

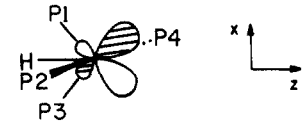

3

With the above results in mind, the observed structure in the present $Fe(H)_2(H_2)(PEtPh_3)_3$ complex is even more surprising. The angle between the two trans phosphines is now down to 149.8 (2)° while the angle between trans H-Fe-P is 177.7 (3)°. The simple extension of the previous analysis would naturally lead to the suggestion that the best conformation should correspond to the H_2 eclipsing the two trans phosphine ligands. Why does H_2 depart from this structure? We now turn our attention to the $Fe(H)_2(H_2)(PEtPh_2)_3$ complex.

The rotational barrier of H_2 in $Fe(H)_2(H_2)(PEtPh_2)_3$ was thus examined: PH_3 was used as a model for the phosphine group. The geometry of the $Fe(H)_2P_3$ (P = PH_3) fragment was held fixed at that found by neutron diffraction. The spatial orientation of the P-H bonds of each PH_3 was taken to be similar to that of the P-C bonds in $PEtPh_2$.

(35) (a) Bachmann, C.; Demyunck, J.; Veillard, A. *J. Am. Chem. Soc.* **1978**, *100*, 2366. Albright, T. A.; Hoffmann, R.; Thibeault, J. C.; Thorn, D. L. *J. Am. Chem. Soc.* **1979**, *101*, 3801. (b) This can be easily deduced from the study of the rotation barrier of olefin in d^4 complexes: Schilling, B. E. R.; Hoffmann, R.; Faller, J. W. *J. Am. Chem. Soc.* **1979**, *101*, 592.

(36) The EHT calculations were done with use of the weighted H_{ij} formula: Ammeter, J. H.; Bürgi, H.-B.; Thibeault, J. C.; Hoffmann, R. *J. Am. Chem. Soc.* **1978**, *100*, 3686. The atomic parameters were taken from the literature: Summerville, R. H.; Hoffmann, R. *J. Am. Chem. Soc.* **1976**, *98*, 7240.

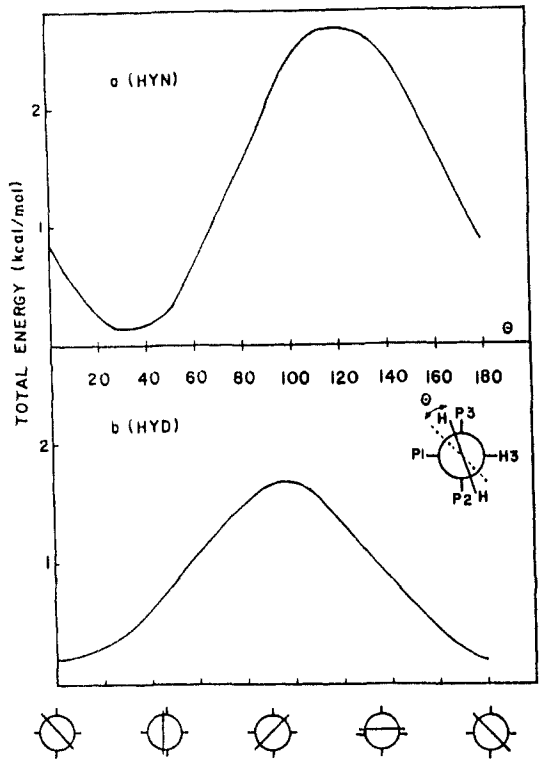

Figure 7. Rotational barrier (in kcal/mol) for H_2 in $Fe(H)_2(H_2)(PH_3)_3$: (a) basis set HYN. (b) basis set HYD. See text.

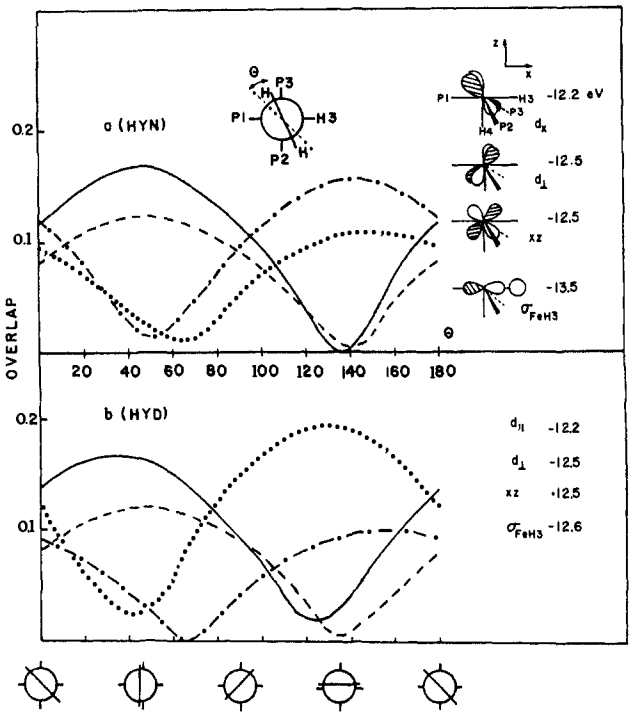

Figure 8. Overlap between σ^*_{HH} and the four highest lying occupied fragment molecular orbitals ($d_\parallel$ (—), $d_\perp$ (– –), xz (–·–), and σ_{FeH3} (···)) of $Fe(H)_2(PH_3)_3$ as a function of θ: (a) basis set HYN. (b) basis set HYD.

Two sets of calculations were done. In the first set, called basis set HYN, the parameters for the H atoms in molecular dihydrogen and in the hydride are the classical parameters for hydrogen (1s orbital with $\zeta = 1.3$ and $H_{ii} = -13.6$ eV). Such parameters actually poorly represent an hydridic (i.e., anionic) center so that in a second set of calculations (basis set HYD) the parameters of the hydride centers ($\zeta = 1.0$, i.e., more diffuse orbital, $H_{ii} = -11.6$ eV, i.e., orbital of higher energy) are different from those of H in molecular dihydrogen. The orientation of H_2 is defined by a rotation angle, θ, with $\theta = 0°$ corresponding to the experimental structure, i.e., H_2 bisecting the P1–Fe–P3 and P2–Fe–H3 angles.

The relative energies as a function of θ are shown in Figure 7a (basis set HYN) and in Figure 7b (basis set HYD). With both basis sets, the rotation barrier is calculated to be small (between 1.5 and 2.5 kcal/mol). Despite the low rotation barrier, a definite region of space, $0° < \theta < 60°$, appears to be more favorable for H_2. For basis set HYN, the preferred conformation is that where H_2 eclipses the P3–Fe–P2 direction[37] ($\theta \approx 40°$, which is the molecular mechanics minimum), but the experimentally observed structure ($\theta = 0°$) is calculated to be only 0.6 kcal/mol higher in energy. For basis set HYD, the experimentally observed structure becomes the most favorable conformation while that for $\theta = 40°$ is now only 0.5 kcal/mol higher in energy. We emphasize that the value of exploring the two sets of hydride parameters is *not* the conclusion of different predicted conformations (since their energies are so similar), but rather that the consistent preference for θ values between 0 and 40° is *independent* of the exact parameters chosen: a broad minimum is expected in this range of conformations. It is also worth noting that for both basis sets, the conformation where H_2 bisects the P3–Fe–H3 and P1–Fe–P2 angles (i.e., $\theta \approx 90°$) is definitely disfavored. This point is of special interest since, if the $Fe(H)_2P_3$ substructure had mirror symmetry, both conformations ($\theta = 0°$ and 90°) would be isoenergetic. This is a consequence of the observed inequivalence of the angles P1–Fe–P2 (97.6 (2)°) and P1–Fe–P3 (105.3 (2)°).

Despite the low rotational barrier, we feel that the results of the calculations clearly indicate electronic control of the experimentally preferred conformation. This is all the more so since molecular mechanics calculations provide no steric preference for $\theta = 0°$. We will now proceed to discuss the factors that cause this preference.

In the $Fe(H)_2P_3$ fragment, the large angles between the phosphine ligands involve bending P2 and P3 back toward H4. This creates a mixing of xy, xz, and yz so that the nonbonding set of the present metal fragment no longer has the simple spatial orientation of an octahedron. As a consequence, simple symmetry arguments are not sufficient to decide the best directions of interaction and we must rely on calculations.

The calculated *overlap* of the occupied σ_{HH} orbital with the three occupied nonbonding orbitals is found to be very small in $Fe(H)_2(H_2)(PH_3)_3$ so that, even in this lower symmetry, *no significant four-electron destabilization* is generated for the eclipsed conformation. The preference for a given structure must thus be determined by the interaction of σ^*_{HH} with the metal fragment. All high-lying occupied metal orbitals that overlap significantly with σ^*_{HH} will play a role in the bonding scheme. This criterion leads us to consider not only the three nonbonding orbitals of the metal but, in addition, the next lower orbital, which is mostly a σ-type Fe–H3 bonding orbital;[38] called σ_{FeH3} for convenience, it is schematically represented in **4**. The three highest occupied

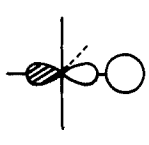

4

d orbitals are represented in Figure 8. It is easy to see how they originate from the nonbonding set of an idealized ML_5 flat square pyramidal fragment (90° angles between ligands). If $Fe(H)_2P_3$ had that idealized geometry, the three highest occupied d orbitals

(37) Although the y axis cannot be precisely aligned with the P3–Fe–P2 direction due to the fact that the P1–Fe–P3 angle is larger than the P1–Fe–P2 angle, we define y as perpendicular to the P1–Fe–H3 plane.

(38) Lichtenberger, D. L.; Darsey, G. P.; Kellog, G. E.; Sanner, R. D.; Young, V. G., Jr.; Clark, J. R. *J. Am. Chem. Soc.* **1989**, *111*, 5019.

would have been *yz*, *xy*, and *xz*. Bending P2 and P3 toward H4 and away from P1 causes *yz* and *xy* to strongly mix together. Two new orbitals are generated. The higher one (destabilized by phosphine lone pairs), $d_{\parallel}$, is located along the extension of P2 and P3 and is significantly hybridized away from the phosphine. Lower in energy, one finds a combination of *yz* and *xy*, $d_{\perp}$, which is approximately perpendicular to the P2–Fe–P3 plane and is therefore more nonbonding than $d_{\parallel}$. Since the P1–Fe–H3 angle is close to 180°, the *xz* orbital remains essentially pure; however, a small rotation around the *z* axis, obtained by mixing some *yz* contribution, is found because of the nonsymmetrical position of P2 and P3, with respect to the *xz* plane. This slight distortion will have some structural consequence as will be described later.

The overlap of σ^*_{HH} with these four fragment molecular orbitals, $d_{\parallel}$, $d_{\perp}$, *xz*, and σ_{FeH3}, is shown in Figure 8, parts a (basis set HYN) and b (basis set HYD). Both basis sets give qualitatively the same results: the difference in the quantitative values will be discussed later on. The overlap with $d_{\parallel}$ is maximum for $\theta = 45°$, where H_2 eclipses the P3–Fe–P2 bonds, and is null for $\theta = 135°$. The overlap with $d_{\perp}$ follows the same variation. It should be noted that in an ideal octahedral complex, the overlap of σ^*_{HH} with a pure *xy* orbital would have been null for all θ values. It is the large mixing between *yz* and *xy* (as a consequence of the non-octahedral $Fe(H)_2P_3$ angles) that is responsible for the non-zero value and the θ dependence. The overlap of σ^*_{HH} with *xz* is largest when H_2 aligns with P1–Fe–H3, but rotation toward $\theta = 0°$ maintains a large overlap. The overlap of σ^*_{HH} with σ_{FeH3} is, as expected, maximal when H_2 aligns with the Fe–H3 bond, $\theta = 135°$ (but it still has large values for a rotation to $\theta = 0° = 180°$). Which of these four interactions dominate? Since $d_{\parallel}$ and $d_{\perp}$ are higher in energy than *xz* and σ_{FeH3}, eclipsing the P2–Fe–P3 may still be the preferred conformation (case of basis set HYD). However, as can be seen in Figure 8a,b, the overlap of σ^*_{HH} with $d_{\parallel}$ and $d_{\perp}$ does not decrease considerably by going from 45° to 0°. In contrast, the overlap with *xz* and σ_{FeH3} increases considerably from $\theta = 45°$ to 0°. Consequently, the conformation with $\theta = 0°$ corresponds to an excellent *compromise* between the four orbitals interacting with σ^*_{HH}, with the result that $\theta = 0°$ is close to the minimum for basis set HYN and even becomes the minimum one using basis set HYD.

(b) Influence of a Cis Ligand on the Rotational Conformation. What is it about the basis set HYD that favors the experimentally observed structure ($\theta = 0°$)? Since the explanation is related to the fluxional behavior of the complex, it is worth addressing this point. A metal–hydride σ bond is mostly localized on the hydride. Since a hydride orbital is considerably more diffuse and higher in energy than a protic type hydrogen center, these features are better represented by the HYD basis set. We now analyze the overlap matrix and the Mulliken Overlap Population to describe the consequence of changing the parameters of the hydrogen center.

Among the four orbitals that are interacting with σ^*_{HH}, the two most important interactions are those made by $d_{\parallel}$ and σ_{FeH3}. The latter orbital becomes of increased importance when the hydridic character is well modeled. This is evident in the considerable increase of the Mulliken Overlap population between σ^*_{HH} and σ_{FeH3} (compare parts a and b of Figure 9). In other words, the σ^*_{HH}, having strong interaction with $d_{\parallel}$ and σ_{FeH3}, attempts to take advantage of both interactions. One should note, at this point, that two positions should be possible for H_2, one where H_2 bisects P3–Fe–P1 and P2–Fe–H3 ($\theta = 0°$ as in the experimental case) and one where H_2 bisects P1–Fe–P2 and P3–Fe–H3 ($\theta = 90°$). According to the calculations, the latter conformation is the less favorable. Looking at Figures 8 and 9, it appears that the interaction of σ^*_{HH} with either $d_{\parallel}$ or σ_{FeH3} is of rather similar magnitude for both conformations. The determining factor is *xz*, which is significantly more involved in bonding with σ^*_{HH} for $\theta = 0°$ than for $\theta = 90°$. Why does *xz* favor $\theta = 0°$ over 90°? This is due to the difference in the P1–Fe–P3 (105.3 (2)°) and P1–Fe–P2 (97.6 (2)°) angles. As mentioned above, the *xz* orbital is not entirely in the *xz* plane. Being the lowest nonbonding orbital, it needs to align to avoid

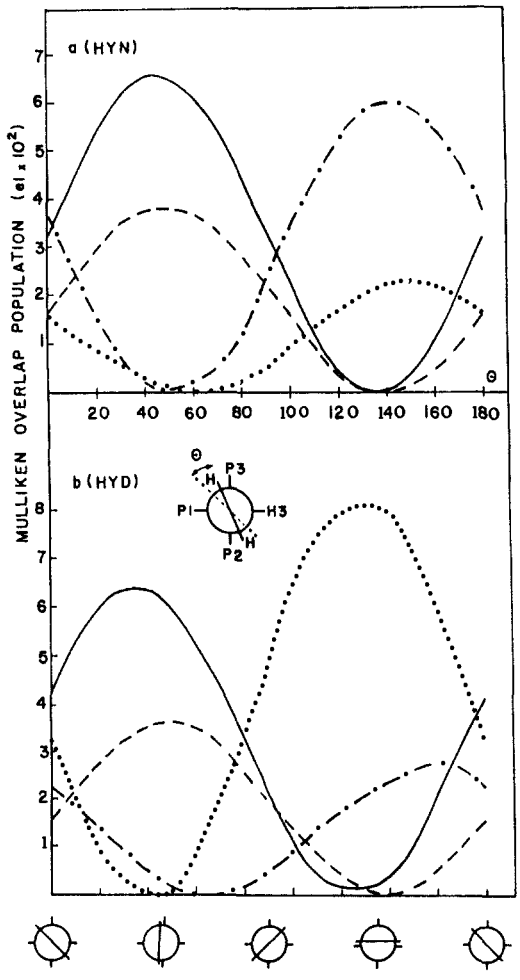

Figure 9. Mulliken Overlap Population between σ^*_{HH} and the four highest lying occupied fragment molecular orbitals ($d_{\parallel}$ (—), $d_{\perp}$ (– –), *xz* (–·–), and σ_{FeH3} (···)) of $Fe(H)_2(PH_3)_3$ as a function of θ: (a) basis set HYN, (b) basis set HYD.

all ligands, so that its best position is perpendicular to the Fe–P3 axis, **5**.

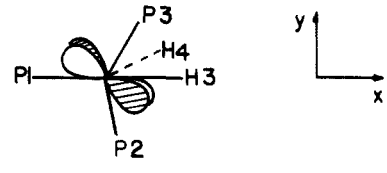

5

When a high-lying d orbital interacts with σ^*_{HH}, electrons are transferred from the metal into the H–H bond. This weakens the H–H bond and corresponds to progress along an oxidative addition reaction path that would ultimately yield a dihydride. When the Fe–H3 bond interacts with a σ^*_{HH} bond, it also transfers electrons into σ^*_{HH} so that it weakens the H–H bond, *simultaneously creating a nascent bond between that hydride and the nearest hydrogen center of the molecular* H_2, as illustrated in **6**.[39] Consequently, not only is the H–H bond weakened, but a new H···H begins to form. This is a very preliminary step toward scrambling H_2 with hydride centers without the necessity of passing through a "classical" tetrahydride $Fe(H)_4P_3$. Continuing along

(39) The Mulliken Overlap Population between H3 and the closest hydrogen of the H_2 ligand at the optimal structure ($\theta = 0°$) is 0.02 with basis set HYD and 0.01 with basis set HYN while the one between the two hydrides is almost nil. Therefore, the situation is different from the H_3 or H_4 complexes studied by Burdett et al. (Burdett, J. K.; Pourian, M. R. *Organometallics* **1987**, *6*, 1684. Burdett, J. K.; Phillips, J. R.; Pourian, M. R.; Turner, J. J.; Upmacis, R. *Inorg. Chem.* **1987**, *26*, 3054).

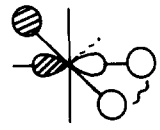

6

the reaction path, a new H_2 molecule is formed and a hydride is left behind. The same process can be repeated between H_2 and one of the two remaining hydrides, **7**.

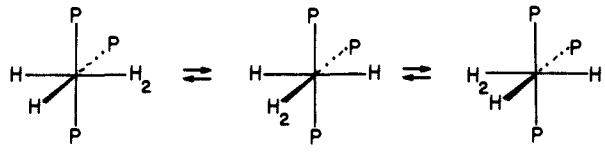

7

A successful analysis of this problem has required consideration of an unusually large number (four) of orbitals on the metal fragment. However, some general features emerge. In the eclipsed structure of $W(H_2)(CO)_3P_2$, the d orbital along the CO axis is lower in energy than the one along the phosphine axis so that the H_2 ligand aligns itself with the metal–phosphine axis. When the four ligands cis to H_2 are equal (e.g., *trans*-$HP_4Fe(H_2)^+$), there is no intrinsic preference for any conformation *as long as* the FeP_4 unit is approximately planar. Essentially free rotation is expected from the calculations. However, any small structural distortion is apparently sufficient to put H_2 in a preferred conformation. In particular, bending two ligands away from H_2 destabilizes the d orbital lying in the plane of the two ligands so that H_2 aligns in that plane, **8**, to maximize back-bonding to σ^*_{HH}. This is the

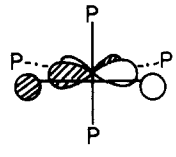

8

case of the $HP_4Fe(H_2)^+$ complex in which one of the angles between two trans phosphines is 167°, while the other one is 172°. Since the metal–phosphine σ-bond is not able to interact with σ^*_{HH} as efficiently (the overlap is smaller and the orbitals of lower energy) as a metal–hydride bond, there is no reason for H_2 to depart from the eclipsing position. In $Fe(H)_2(H_2)P_3$, however, the bending of two phosphines attracts H_2 into that plane but the presence of a cis hydride favors H_2 eclipsing the metal–hydride bond. A compromise is thus struck with H_2 midway between these two competing conformations. Other geometrical distortions (e.g., unequal P1–Fe–P2 and P1–Fe–P3 angles) are responsible for the choice between the two staggered conformations ($\theta = 0°$ vs $\theta = 90°$).

Despite the calculational complexity of the $Fe(H)_2(H_2)P_3$ system, detailed calculations have brought to light the potentially general phenomenon of *cis*-H/H_2 interactions as a factor influential for both H_2 rotational conformation and H-ligand fluxionality. Why is a hydride so uniquely suited to interact with H_2? The reason seems to be a combination of high-lying energy, absence of directionality in the bonding of a 1s orbital with any neighboring orbital, and geometrical proximity, the latter enhanced by the high coordination numbers frequently found in polyhydride compounds. Similar consideration in polyhydride complexes explains their considerable fluxionality.

Summary and Conclusions

Our EHT calculations show a preference for the staggered structure when we better describe the hydridic character of the two hydrides. However, the conformation in which H_2 eclipses the two transoid phosphines remains close in energy. The molecular mechanics calculation indicates that this same eclipsed conformation is also the least crowded. If, in addition, one takes into account that a rigid rotation was assumed both for the EHT and molecular mechanical calculations (this means that the barrier calculated with optimization of all structural parameters should be smaller than the 2 kcal/mol calculated from each method in the "frozen" model), it is safe to conclude that the potential between 0° and 45° is rather flat and that the experimentally observed structure lies in this flat region.

What is the "best" way to merge the rotational barrier from both the EHT and the molecular mechanics calculations? The molecular mechanics calculations have incorporated a better representation of the bulkiness of the phosphine ligands while the EHT calculations were carried out with the simplest model, PH_3. One might think that a simple addition of both curves might give a better estimate of the rotational barrier. Such a procedure was used in the case of $W(H_2)(CO)_3P_2$ in which a too small rotational barrier calculated by ab initio calculations ($P = PH_3$) was increased by addition of the rotational barrier obtained from molecular mechanics calculations.[29] The resulting barrier was in better agreement with the experimental determination. However, quantitative estimation of the back-donation, which is at the origin of the rotational barrier, is underestimated at the SCF level.[40] This might be in large part at the origin of the artificially low barrier from these ab initio calculations.[1b,29] However, the barrier might be overestimated by adding ab initio and molecular mechanics calculations in a one-to-one manner since steric interactions are already in a good part incorporated into the ab initio calculations even though PH_3 was used as a model for the experimental phosphine. In our case, we have precedent from the study of $(CO)_3P_2W(H_2)$ ($P = PH_3$) in which EHT calculations give a reasonable, although slightly overestimated, value of the experimental rotation barrier.[1a,41] We therefore suggest that in the present complex it should not be necessary to add the contribution from the molecular mechanics calculations. We thus estimate the rotation barrier of H_2 to be about 2 kcal/mol with a flat valley between 0° and 45°. Considering the limitations of the calculations, this is in satisfactory agreement with the experimental determination.

The surprising structure of $Fe(H)_2(H_2)P_3$ has revealed that the rotational conformation of a single-faced acceptor ligand (i.e., H_2) can be determined by factors other than back-donation from the d block. In particular we offer evidence for an attractive interaction between H_2 and a neighboring hydride ligand which *opposes* the effect of the metal d block in the present case and lies at the origin of this unprecedented structure. A cis interaction is an effect that, with few exceptions,[2b,42] has not been widely considered in the analysis of structure and reactivity of metal complexes. This interaction is energetically small and is anticipated to play a role primarily under specialized conditions: weak or nearly isotropioc d effects. It appears that hydride centers might be the best candidate for such ligand–ligand attraction due to the fact that they can be at close proximity to the other ligand (e.g., H_2 or olefin[2b]) and that they can overlap with ligands in all directions due to the spherical nature of the 1s orbital.

The barrier for rotation of η^2-H_2 in $W(H_2)(CO)_3(PCy_3)_2$ has been determined by low-frequency inelastic neutron scattering spectroscopy to be 760 cm^{-1} (2.2 kcal/mol), compared to the lower value of 425 cm^{-1} (1.2 kcal/mol) found here by the same method. In $Fe(H_2)(H)_2(PEtPh_2)_3$ there exists a competition between the

(40) Antolovic, D.; Davidson, E. R. *J. Am. Chem. Soc.* **1987**, *109*, 5828. Lüthi, H. P.; Siegbahn, P. E. M.; Almlöf, J. *J. Phys. Chem.* **1985**, *89*, 2156. Lüthi, H. P.; Siegbahn, P. E. M.; Almlöf, J.; Faegri, K., Jr.; Heiberg, A. *Chem. Phys. Lett.* **1984**, *111*, 1. Dedieu, A.; Nakamura, S.; Sheldon, J. C. *Chem. Phys. Lett.* **1987**, *141*, 323. Dedieu, A.; Sakaki, S.; Strich, A.; Siegbahn, P. E. M. *Chem. Phys. Lett.* **1987**, *133*, 317. Moncrieff, D.; Ford, C. P.; Hillier, I. H.; Saunders, V. R. *J. Chem. Soc., Chem. Commun.* **1983**, 1108. Koga, N.; Jin, S. Q.; Morokuma, K. *J. Am. Chem. Soc.* **1988**, *110*, 3417.

(41) The metal–H bond distance was taken too short in ref 1a. However, no real change in the calculated energy barrier is found by taking the correct distance.

(42) Fenske, R. F.; DeKock, R. L. *Inorg. Chem.* **1970**, *9*, 1053. Marsella, J. A.; Curtiss, C. J.; Bercaw, J. E.; Caulton, K. G. *J. Am. Chem. Soc.* **1980**, *102*, 7244. Volatron, F.; Eisenstein, O. *J. Am. Chem. Soc.* **1986**, *108*, 2173.

influence of the d block, which favors eclipsing of the P-Fe-P plane, and an attractive cis interaction between H_2 and the adjacent Fe-H bond. Consequently, $Fe(H_2)(H)_2(PEtPh_2)_3$ shows a broad minimum, and thus the maximum is necessarily lower: these competing factors tend to stabilize conformers even when away from their individual minima, thereby lowering the barrier due to either factor alone (in comparison to $W(H_2)(CO)_3(PCy_3)_2$).

Acknowledgment. This work was supported by the U.S. NSF and DOE, the French CNRS, and the European Economic Community. Work at Brookhaven was carried out under contract DE-AC02-76CH00016 with the U.S. Department of Energy, Office of Basic Energy Sciences. Work at Los Alamos was performed under the auspices of the U.S. Department of Energy, Division of Chemical Sciences, Office of Basic Energy Sciences. O.E. acknowledges the Indiana University Institute for Advanced Study for a fellowship. The work has also benefited from the use of facilities at the Los Alamos Neutron Scattering Center, a national user facility funded as such by the Department of Energy, Office of Basic Energy Sciences. The Laboratoire de Chimie Théorique is associated with the CNRS (URA 506) and is a member of ICMO and IPCM. We thank Scott Horn of the Indiana University Molecular Structure Center and H. Blank of the Institut Laue-Langevin for skilled technical assistance. David Rathjen for his help during the neutron diffraction measurements, and Ilpo Mutikainen for valuable discussions.

Supplementary Material Available: Tables of full crystallographic details and anisotropic thermal parameters for $FeL(H)_2(PEtPh_2)_3$, where $L = H_2$ and N_2 (4 pages); listing of observed and calculated structure factors (77 pages). Ordering information is given on any current masthead page.

Do Nonclassical Silabenzene Anions Exist? Synthesis and X-ray Crystal Structure of Crown Ether Stabilized Lithium Silacyclohexadienides, $Li(12\text{-crown-}4)_2Me_2SiC_5H_5$ and $Li(12\text{-crown-}4)_2\text{-}t\text{-}Bu(H)SiC_5H_5$

Peter Jutzi,*,† Marion Meyer,† H. V. Rasika Dias,‡ and Philip P. Power‡

Contribution from the Faculty of Chemistry, University of Bielefeld, 4800 Bielefeld, Universitätsstrasse, F.R.G., and Department of Chemistry, University of California, Davis, California 95616. *Received December 4, 1989*

Abstract: Metalation of 1,1-dimethyl-1-silacyclohexa-2,4-diene (**10**) and 1-*tert*-butyl-1-hydro-1-silacyclohexa-2,4-diene (**11**) with *n*-butyllithium leads to the corresponding silacyclohexadienyl lithium compounds, which on further treatment with the crown ether 12-crown-4 afford the deep red to violet crystalline title compounds $[Li(12\text{-crown-}4)_2][Me_2SiC_5H_5]$ (**12**) and $[Li(12\text{-crown-}4)_2][t\text{-}Bu(H)SiC_5H_5]$ (**13**) as solvent-separated ion pairs with free silacyclohexadienide anions. The question whether the anions in **12** and **13** may be regarded as silicon-bridged pentadienide species or as nonclassical silabenzenes is answered on the basis of ^1H, ^{13}C, ^{29}Si NMR, and IR data of **10**–**13** and on the basis of an X-ray crystal structure determination of **12**. The π-bonding in these $R_2SiC_5H_5^-$ anions is found as quasiaromatic. In this context, the most intriguing structural and spectroscopic features are as follows: (I) planarity of the SiC_5 framework, short endocyclic silicon–carbon bonds, and rather long exocyclic Si–C bonds in **12**. (II) NMR signals for the ring-carbon hydrogens in **12** and **13** at comparatively low field. (III) dramatic low field shift in the ^1H NMR spectrum for the Si–H proton on going from **11** to **13**, and (IV) shift to lower wave numbers for the Si–H stretching mode (IR) and smaller Si–H coupling constant (^{29}Si NMR) on going from **11** to **13**. The π-bonding in $R_2SiC_5H_5^-$ anions is qualitatively rationalized using the MO model (interaction of π-pentadienide with σ^*SiR_2 orbitals, negative hyperconjugation) and the valence bond approach (participation of the resonance structures **8c**, **8d**).

In phosphorus and sulfur chemistry, two different types of benzene-like heteraromatic compounds have attracted widespread interest during the last 30 years. First, there are the classical $(p\text{–}p)\pi$ systems with sp^2 hybridized heteroatoms such as the λ^3-phosphabenzenes **1**[1] and the isoelectronic thiapyrylium cations **2**.[2] The aromatic character of these compounds is now broadly accepted by both experimentalists and theoreticians. In contrast, the second group of compounds, the so-called nonclassical π systems involving four coordinate heteroatoms, has generated considerable controversy. Examples of these compounds include the λ^5-phosphabenzenes **3**[3] and the isoelectronic neutral thiabenzenes **4**.[4] The bonding discussion on these heterocyclic π systems has focused on the degree of participation by the heteroatom center in the delocalization through $(p\text{–}d)\pi$-overlap. Currently available experimental observations appear to rule out any bonding proposal [**3a**, **4a**] where appreciable π electron density is transferred from the carbon to the heteroatom in **3** and **4**. These compounds are best described as cyclic phosphonium or sulfonium ylides, as indicated in **3b** and **4b**. The experimental results in favor of **3b** and **4b** mainly involve X-ray crystal structure investigations and NMR data.

Conjugative electron donation from a carbon p orbital to a sp^3 hybridized heteroatom cannot, in principle, be ruled out. In fact, recent publications have postulated that cyclic conjugation exists in the phosphirenium cation **5**[5] and in the phosphadiboretane **6**.[6]

†University of Bielefeld.
‡University of California.

(1) (a) Dimroth, K. *Fortschr. Chem. Forsch.* **1973**, *38*, 1. (b) Ashe, A. J., III; Sharp, R. R.; Tolon, J. W. *J. Am. Chem. Soc.* **1976**, *98*, 5451. (c) Ashe, A. J., III *Acc. Chem. Res.* **1978**, *11*.
(2) Yoneda, S.; Sugimoto, T.; Yoshida, Y. *Z. Tetrahedron* **1973**, *29*, 2009.
(3) Dimroth, K. *Acc. Chem. Res.* **1982**, *15*, 61.
(4) Maryanoff, B. E.; Stackhouse, J.; Senkler, G. H., Jr.; Mislow, K. *J. Am. Chem. Soc.* **1975**, 2718.
(5) Vural, J. M.; Weissmann, A.; Baxter, S. G.; Cowley, A. H.; Nunn, C. M. *J. Chem. Soc., Chem. Commun.* **1988**, 462.
(6) Berndt, A.; Klusik, H.; Pues, C.; Wehrmann, R.; Meyer, H.; Lippold, U.; Schmidt-Lukasch, G.; Hunold, R.; Baum, G.; Massa, U. *Boron Chemistry*; Proceedings of the 6th International Meeting on Boron Chemistry (IMEBORON), Hermanek, S., Ed.; World Scientific Press.

0002-7863/90/1512-4841$02.50/0